Adsorption of Cs on H-precovered W(110) surfaces

C. A. Papageorgopoulos
Department of Physics, University of Ioannina, P.O. Box 1186, GR-452 10 Ioannina, Greece
(Received 11 July 1988; revised manuscript received 12 April 1989)

Deposition of Cs on clean W(110) at room temperature produces a single layer with a compressed hcp structure and gives the characteristic work-function curve of alkali-metal atoms on metals which goes through a minimum value (ϕ_{min}), and a subsequent maximum (ϕ_{max}) at saturation Cs coverage. During Cs deposition on hydrogenated W(110) the Cs atoms form an independent overlayer. The presence of a H underlayer weakens the bond and increases the ordering of the Cs atoms. Cesium forms a $p(2\times2)$ structure and a compressed hcp structure on 0.5 monolayers (ML) of H, whereas on 1 ML of H, it forms an oblique (3×1) structure. Also, the preadsorption of H causes (i) an increase of the initial dipole moment, (ii) a lowering of ϕ_{min}, (iii) a shift of the ϕ_{min} to smaller Cs coverage Θ_{Cs}, and (iv) an increase of ϕ_{max}. These are attributed to an increase of the Cs-W interlayer distance by the preadsorbed hydrogen, which restricts the electronic communication between Cs and the W substrate with a consequence an increase of metallization in the Cs overlayer. This explanation is consistent with results of theoretical calculations.

I. INTRODUCTION

The interest in the coadsorption of alkali metals and gases on semiconducting and metallic substrates increases continuously. Among the alkali-metal elements, Cs is the most widely used. It is reactive and strongly affects the surface electronic properties.

Coadsorption of Cs and O_2 on metallic and semiconducting substrates provides low-work-function surfaces.[1-3] This can be used in making photocathodes and thermionic energy converters.[4,5] Submonolayers of Cs can be used as catalysts in the oxidation of semiconductors, especially in the formation of Si/SiO_2 interfaces of high technological importance.[6,7] Cesium is also used in many other chemical reactions, such as $H_2O+CO \rightarrow CO_2+H_2$ for H_2 production.[8] Recently, cesiated transition-metal surfaces such as those of tungsten and molybdenum have been used for the production of negative hydrogen ions.[9]

These systems are characterized by a low work function, a low H sticking coefficient,[10,11] and a high yield of backscattered and sputtered negative ions.[12,13] Beams of energetic H^- ions are needed for neutral-beam heating of future fusion plasmas.[14] The formation of H^- ion in the H-Cs/W surface collision is affected strongly by the adsorption of hydrogen atoms.[15] However, the actual mechanism of this effect has not been explained completely. This is reasonable, since the coadsorption of Cs and H_2 on metallic substrates is not yet understood.

According to our previous reports of Cs and H_2 coadsorption on W(100) and Mo(110), the sticking coefficient of H_2 alone on these surfaces is fairly high.[10,11] When a small amount of Cs was deposited on clean W(100) and Mo(110) surfaces, the sticking coefficient of subsequently adsorbed hydrogen decreased drastically. Work-function measurements showed that the work function at maximum coverage of Cs on W(100), ϕ_{max}, was increasing with increasing amounts of preadsorbed hydrogen.[10] These data also showed that the work-function minimum ϕ_{min}, which was measured before the completion of a Cs monolayer on clean W(100), was shifted to smaller values of Cs coverage with increasing amount of preadsorbed hydrogen. The increase of ϕ_{max} was correlated to the increase of work function during hydrogen adsorption on clean W(100).[10] Unlike W(100), the work function of W(110) was decreasing upon hydrogen absorption at 300 K.[16,17] This basic difference of the behavior of H on clean W(100) and W(110) surfaces prompted questions which initiated the present work of Cs and H_2 coadsorption on a W(110) surface. Moreover, a W(110) surface covered with a submonolayer of Cs has promising characteristics for negative-ion formation.[14]

The present paper deals with the study of Cs deposition on H precovered W(110) surfaces. These studies prerequire detailed knowledge of the separate adsorption of H_2 and Cs on clean W(110). The results are compared with related reported studies.

II. EXPERIMENT

The experiments were performed in a UHV system equipped with surface analysis techniques for low-energy electron diffraction (LEED), Auger-electron spectroscopy (AES), thermal-desorption spectroscopy (TDS) and work-function (WF) measurements. The TDS measurements were made with a quadrupole mass spectrometer capable of detecting mass to charge ratios up to 300. The WF changes were measured with a Kelvin probe. Absolute work functions were obtained by assuming a clean W(110) work-function value of 5.3 eV.[18]

The W(110) specimen ($15\times6\times0.15$ mm^3) could be resistively heated up to 2500 K. The crystal temperatures were measured by a W-Re thermocouple attached at the back side of the crystal. The specimen was cleaned in the vacuum system by heating to $\sim$1300 K in O_2 at

10^{-7} Torr with intermediate flashings to 2500 K. Auger measurements were used to following the cleaning of the crystal.

Spectroscopically pure H_2 was admitted to the system through a bakable leak valve. Atomic cesium was deposited from a Knudsen fusion cell containing metallic cesium (99.99% pure). A leak valve prevented the spreading of cesium over the rest of the chambers while a shutter was used to accurately dose the specimen with Cs. A rotatable surface ionization detector with a Pt ionizer could be moved into a position in front of the Cs source to determine the Cs flux, which was kept constant at $7.4\times10^{12}\,cm^{-2}s^{-1}$.

III. SEPARATE ADSORPTION OF HYDROGEN AND CESIUM

A. H_2 on clean W(110)

As we mentioned in the Introduction, the study of the coadsorption of H_2 and Cs on W(110) prerequires detailed knowledge of the behavior of each adsorbate alone on clean W(110).

Adsorption of hydrogen on W(110) has been reported in many instances.[16,17,19] Most of the measurements have been repeated in this work. Except for an increase in background, adsorption of hydrogen on W(110) at room temperature (RT) does not produce any extra diffraction feature in the LEED pattern.

Thermal desorption results indicate that hydrogen on clean W(110) has two adsorption states β_1 and β_2. These results will be shown later in this paper in correlation with the hydrogen-desorption spectra from Cs/H/W(110). The first adsorption state β_2 of hydrogen on W(100) corresponds to $\Theta_H=0.5$ (which requires about 3 L of hydrogen exposure) and the H atoms occupy three-fold sites of the W(110) substrate. [1 langmuir (L)$\equiv10^{-6}$ Torr s.] Above 0.5 monolayers (ML), the hydrogen atoms reside on top of the W atoms of the substrate and constitute the second adsorption binding state β_1.[17]

Our measurement of the work-function variation of a clean W(110) surface upon hydrogen adsorption at RT is not shown here because it is quite similar to that reported by Herlt and Bauer.[17] Adsorption of hydrogen on a W(110) surface causes a decrease in WF by 0.5 eV, in contrast to the W(100) surface, where the work function increases with hydrogen adsorption.[10] This basic difference may result a different behavior of Cs on H/W(100) and H/W(110) surfaces and will probably help to understand the mutual effects of Cs and H on W substrates.

B. Cs on clean W(110)

Figure 1 shows the Auger peak height of Cs (560 eV), W (170 eV), and WF versus Cs deposition time at RT. Initially, the Auger peak height of the W substrate decreases linearly, while that of Cs increases linearly with Cs deposition and both approach a plateau at the time when the WF reaches its maximum value. This indicates

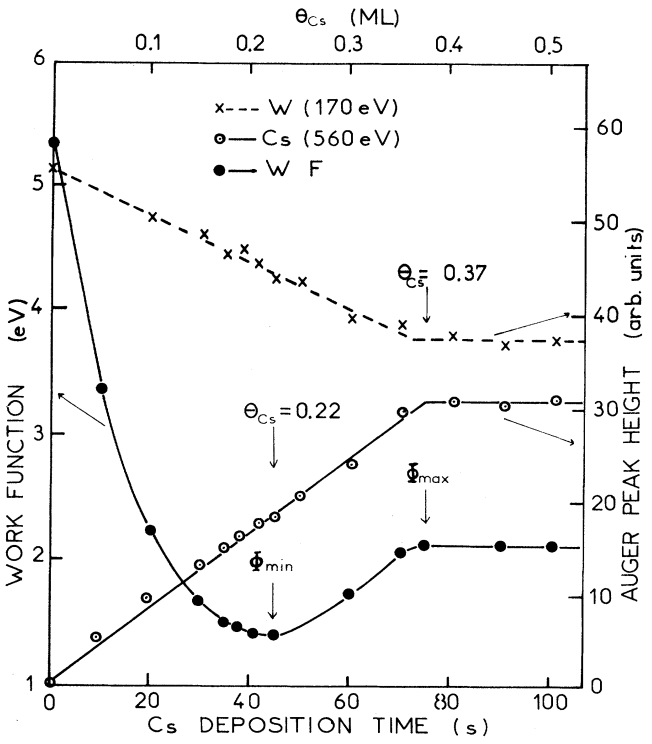

FIG. 1. Work function and Auger peak heights of Cs (560 eV) and W (170 eV) vs Cs deposition time on W(110) surfaces at RT.

that Cs is deposited uniformly in a single monolayer and does not form a second layer on W(110) at RT, in contrast to W(110) at low temperatures (LT), where Cs grows a second layer.[2,20] As is seen in Fig. 1, deposition of Cs on W(110) gives the characteristic WF curve of Cs on metal surfaces.[1,2,21] Initially the WF decreases with Cs deposition, it goes through a minimum value $\phi_{min}=1.4$ eV at $\Theta_{Cs}=0.22$ ML, and subsequently increases to a maximum value $\phi_{max}=2.15$ eV at $\Theta_{Cs}=0.37$ ML, saturation coverage of Cs. The Cs coverage could be calculated from the Cs flux. The calculations agree quite well with the correlation of LEED, AES, and WF measurements and also with published work.[2]

Fedorus and Naumovets[20] reported a sequence of LEED patterns during depositions of Cs onto the W(110) surface which was cooled to 77 K. In the present work, the W(110) substrate is kept at RT. Initial deposition of Cs on clean W(110) is indicated by an increase of background in the LEED pattern, without showing any extra ordered Cs structure, as it does at LT.[20] Near saturation coverage the background is resolved into a hexagonal close-packed (hcp) pattern with split beams, shown in Fig. 2(b). The scheme of spot location is given in Fig. 3(b). Further deposition of Cs does not cause any change in the pattern. This pattern is similar to that which was observed during the completion of the first monolayer of Cs on W(110) at 77 K.[20]

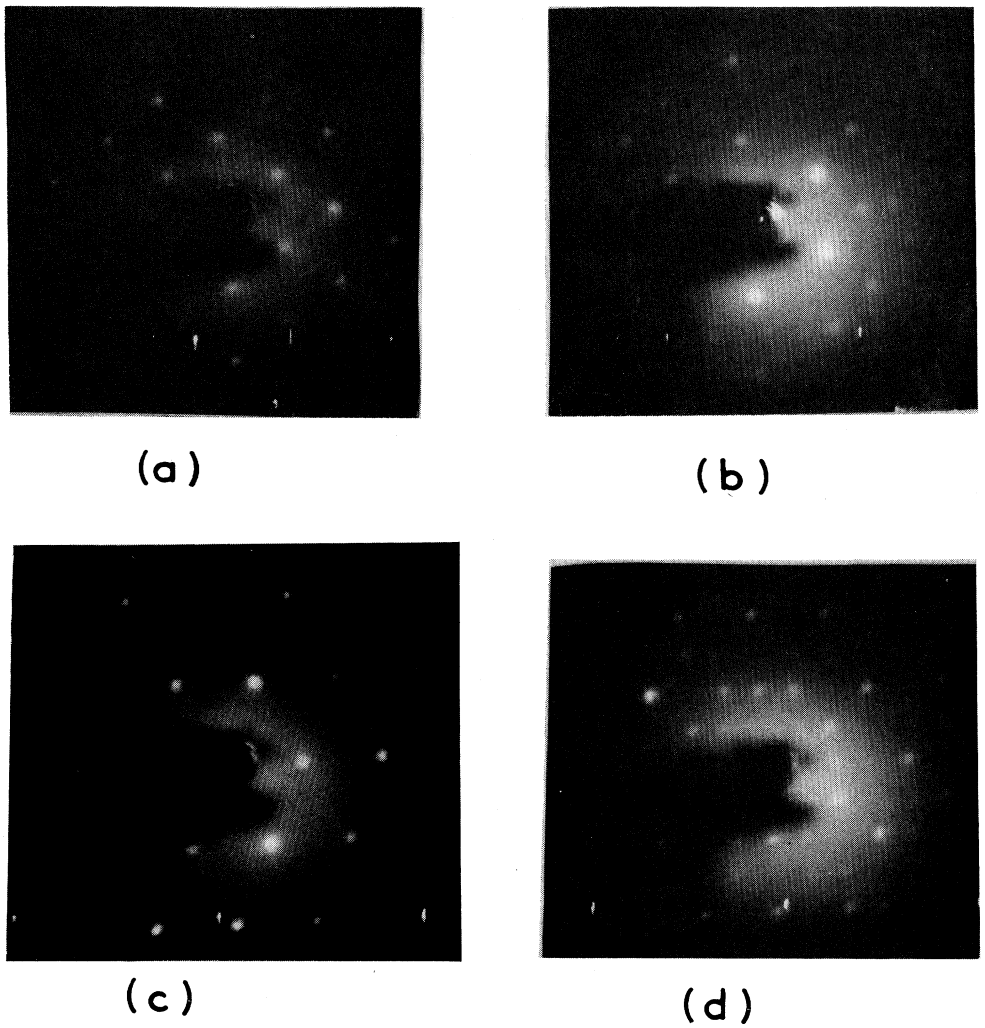

FIG. 2. LEED patterns of Cs on H-covered W(110) at RT. (a) $p(2\times2)$Cs, $\Theta_{Cs}\approx0.25$, $\Theta_H\approx0.5$ (95 eV). (b) hcp pattern with split beams $\Theta_{Cs}\approx0.37$, $\Theta_H\approx0.5$ [this pattern is similar to that of saturated Cs on clean W(110)] (85 eV). (c) Oblique (3×1)Cs, $\Theta_{Cs}\approx0.33$, $\Theta_H\approx1$ (95 eV). (d) Superposition of hcp and oblique (3×1)Cs, $0.33<\Theta_{Cs}<0.37$, $0.5<\Theta_H<1$, 100 eV.

IV. CESIUM ADSORPTION ON HYDROGENATED W(110)

A. LEED observations

As we mentioned earlier, the preadsorbed hydrogen on W(110) at RT does not produce any extra LEED pattern. Also, the adsorption of Cs on clean W(110) at RT does not produce any extra LEED pattern other than the hcp pattern at saturation coverage.

$\Theta_H\leq0.5$. Deposition of Cs on W(110) which is covered with $\Theta_H\leq0.5$ ML of hydrogen at RT produces a (2×2) LEED pattern, shown in Figs. 2(a) and 3(a). This pattern has its maximum intensity at $\Theta_{Cs}\sim0.25$ ML and, most likely, is due to the Cs overlayer. As the Cs coverage increases, the pattern changes to a hcp pattern, except that the background is higher now. This pattern is similar to that [Figs. 2(b) and 3(b)] produced on clean W(110) at saturation Cs coverage ($\Theta_{Cs}\sim0.37$ ML). The formation of the (2×2) structure of Cs, which is not observed on clean W(110) at RT, indicates that the preadsorbed hydrogen increases the ordering of the Cs overlayer at low Cs coverage. The presence of H between Cs and W probably weakens the Cs-W interaction, with a consequent predomination of the Cs-Cs interaction.

$\Theta_H\simeq1$. Deposition of Cs on W(110) covered with $\Theta_H\sim1$ ML of hydrogen at RT gives a very good oblique (3×1) LEED pattern at saturation Cs coverage [Figs. 2(c) and 3(c)]. According to this pattern, Cs on 1 ML of preadsorbed H on W(110) saturates at about 0.33 ML.

It appears that when the hydrogen of both binding states is present on the surface, the maximum amount of Cs that can be deposited at RT is less than that which can be deposited on a clean W(110) surface or a W(110) surface covered by ≤0.5 ML of hydrogen.

$0.5<\Theta_H<1$. When the W(110) is completely covered

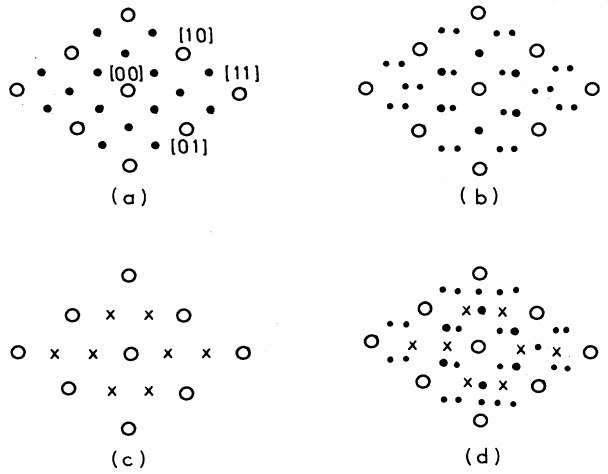

FIG. 3. Schemes of spot location of the respective *a*, *b*, *c*, and *d* patterns in Fig. 3.

with hydrogen of the β_2 adsorption state and partially covered with hydrogen of the β_1 state, the Cs overlayer at saturation coverage forms a superposition of the hcp and the oblique (3×1) LEED pattern [Figs. 2(d) and 3(d)]. The hcp structure is produced on areas precovered only with the β_2 state, while the oblique (3×1) structure is produced on areas precovered with hydrogen of both β_1 and β_2 states. Such a superposition implies that, before the completion of 1 ML, hydrogen atoms of the β_1 state form islands.

When the surface with the oblique (3×1) structure of Cs is heated to 450 K for ≤ 1 min most hydrogen of the β_1 state and part of the Cs overlayer are removed from the surface and the Cs structure changes to a very good (2×2) structure. This structure is similar to that which has been observed with about 0.25 ML of Cs on 0.5 ML of preadsorbed H (β_2) on W(110).

Figure 4 shows the structural models of the LEED patterns (a), (b), and (c) of Fig. 2. According to Ref. 17, the hydrogen atoms of the β_2 state ($\Theta_H=0.5$) reside on threefold sites, as indicated by the small solid circles. The Cs coverage of 0.25 ML, which does not show any extra LEED pattern on clean W(110) at RT, forms a well-ordered $p(2\times2)$ structure on 0.5 ML of hydrogen. The Cs atoms are located in the troughs which are formed by the rows of H atoms and most likely are displaced away from the W substrate by the H atoms. The arrangement of Cs atoms in the $p(2\times2)$-Cs structure should not cause any removal of H atoms from their initial binding states. The $p(2\times2)$ structure of Cs is the initial stage of the close-packed structure. With increasing coverage, the Cs atoms move along the [001] direction to form the final close-packed structure of Fig. 4(b). The latter structure is similar to that of Cs on clean W(110) at RT. This indicates that the Cs atoms form an independent layer on top of hydrogen. This is quite similar to the behavior of Cs on hydrogenated W(110).[1]

When the coverage of H is 1 ML there are H atoms of both β_1 and β_2 binding states on W(110). As is shown in Fig. 4(c), the atoms of the β_1 state reside on top of the W atoms. In the presence of H of both β_1 and β_2 states, the arrangement of the Cs atoms is different than that on clean W(110) or on W(110) covered by 0.5 ML of H.

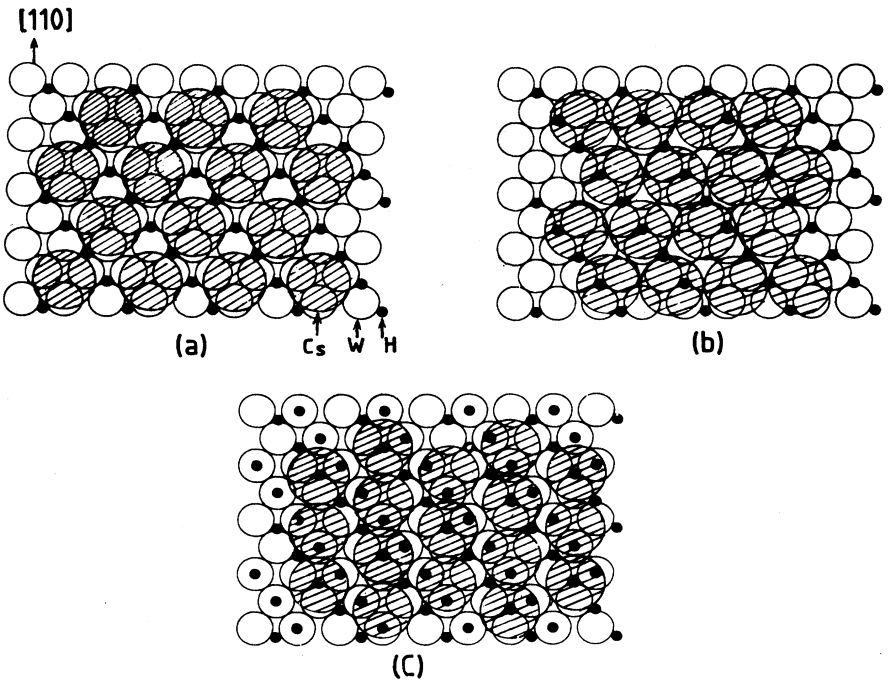

FIG. 4. The structural models of the LEED patterns (a), (b), and (c) shown in Fig. 2.

Now, the Cs atoms are aligned with the rows of the H underlayer and form the closest possible structure allowed by the H. The oblique (3×1) structure corresponds to $\Theta_{Cs}=0.33$, which is smaller than that on 0.5 ML of H. [If the W atoms of W(110) surface formed a perfect hexagonal arrangement, the Cs structure in Fig. 4(c) would be $(\sqrt{3}\times\sqrt{3})R30°$.] As is indicated in Fig. 3(c), the Cs atoms are obviously above H atoms and the displacement away from the surface is greater than that on 0.5 ML of H [Fig. 4(b)] since H atoms of the β_1 state reside on top of the W atoms.[17] The arrangement (imposed by the H underlayer) of the Cs atoms in the oblique (3×1) structure shown in Fig. 4(c) supports the argument that H atoms remain in the initial binding sites.

B. WF measurements

Figure 5 shows the WF versus Cs deposition time on clean W(110) and H-covered W(110) surfaces.

In each of these curves there is an initial WF minimum ϕ_{min} and a subsequent maximum ϕ_{max} at saturation Cs coverage. As is seen in the figure, ϕ_{min} is lowered and shifted to smaller Cs coverage with increasing amounts of preadsorbed hydrogen. Moreover, the increase of the initial hydrogen coverage causes ϕ_{max} to increase. These measurements are quite similar to those of Cs on H-covered W(100) surfaces.[10] However, due to the lack of other correlated techniques such as AES and TDS, the explanation of the WF results was difficult. An explanation of the lowering of ϕ_{min} with increasing amounts of preadsorbed H was based on the theory of the work function by Lang and Kohn.[22] However, there was no satisfactory explanation given in Ref. 10 for the increase of ϕ_{max} and the shift of ϕ_{min} to lower Cs coverage with increasing amounts of preadsorbed H. A possible cause of the ϕ_{min} shift could be an increase of the sticking coefficient of Cs with increasing amounts of preadsorbed H on W(110). However, this possibility should not be considered because, first, it is generally believed that before ϕ_{min}, the sticking coefficient of Cs on metals is very close to 1, and second, the following AES and TDS measurements do not indicate any change of Cs sticking coefficient in the presence of H on W(110).

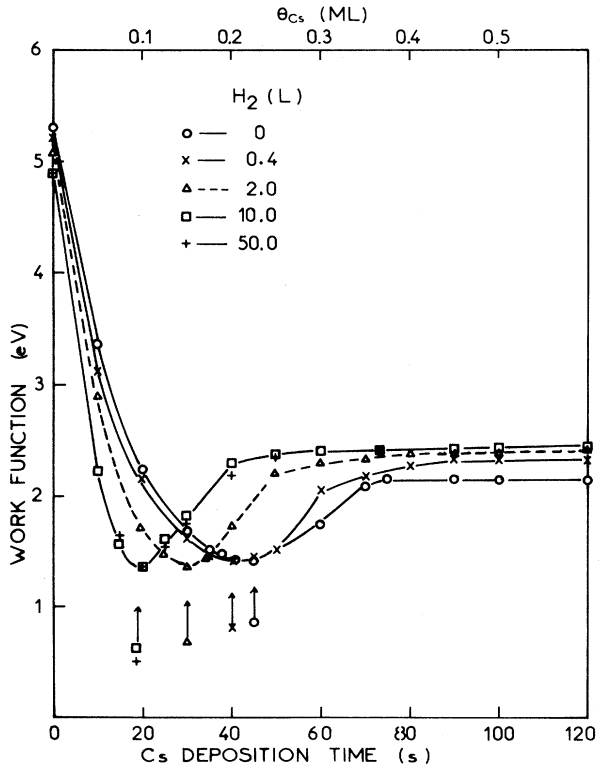

FIG. 5. Work function vs Cs deposition time on clean and H-covered W(110) surfaces.

C. AES measurements

Figure 6 shows the variation of Cs (560 eV) peak height versus deposition time of Cs on H-covered W(110) surfaces are compared to that on clean W(110). The almost linear variation of these curves suggests that the adsorption of Cs on H/W(110) is uniform, in agreement with LEED observations. The important massage of this figure is that the presence of H on the W(110) surfaces does not cause any substantial change in the sticking coefficient of Cs on the surface. This is important because it precludes the attribution of the shift of ϕ_{min} (Fig. 5) to a change in sticking of Cs with increasing amounts of preadsorbed H. Near saturation coverage, the peak height decreases slightly as the amount of preadsorbed H increases. This is consistent with the observation that the maximum amount of Cs that can be deposited on W(110) at RT decreases with increasing amounts of predeposited H.

D. TDS measurements

1. TDS of Cs

Figures 7(a) and 7(b) show two series of thermal desorption spectra of Cs from Cs/W(110) and Cs-covered

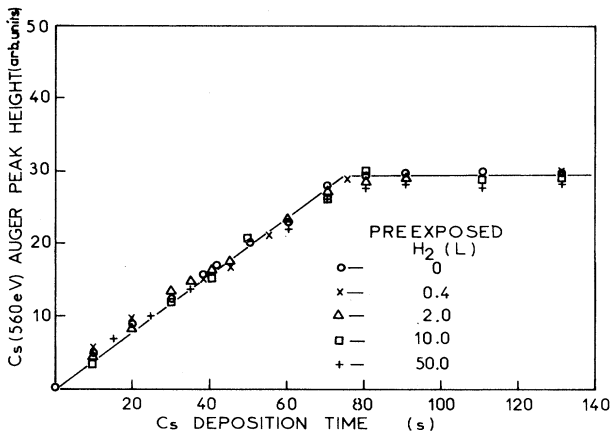

FIG. 6. Auger peak height of Cs (560 eV) vs Cs deposition time on H-covered W(110) surfaces.

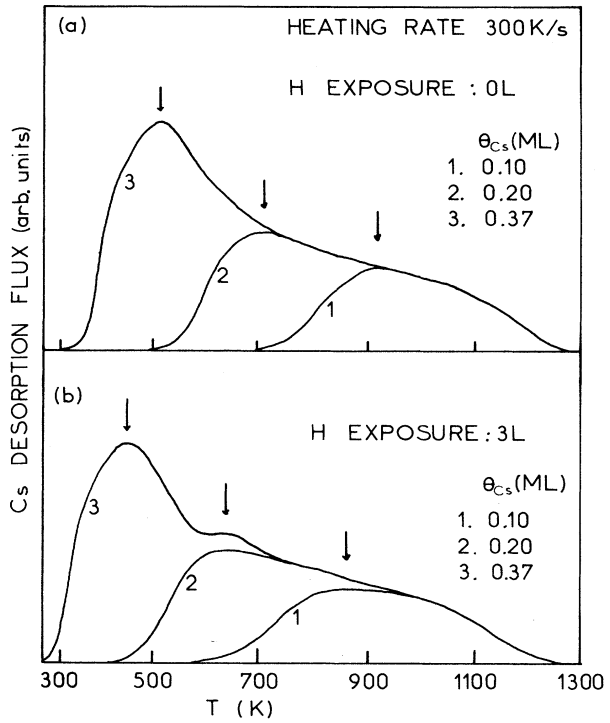

FIG. 7. TDS of Cs from (a) Cs/W(110) and (b) Cs-covered H/W(110) surfaces.

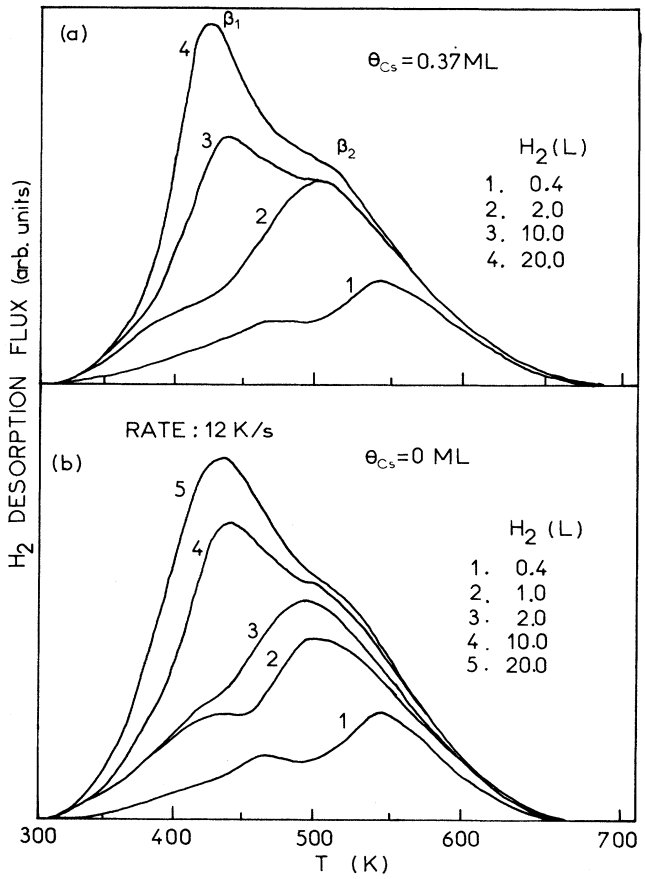

FIG. 8. TDS of H_2 from (a) Cs-covered H/W(110) and (b) H/W(110) surfaces.

H/W(110) surfaces, respectively. The spectra in Fig. 7(a) are similar to those reported previously.[2] The heating rate of the substrate during Cs desorption was ~ 300 K s^{-1}. The relatively fast heating rate was necessary to minimize diffusion of Cs out of the specimen area sampled by the mass spectrometer. Neutral desorption spectra from Cs/W(110) indicate a rather continuous decrease of the desorption energy as the Cs coverage increases. These spectra are shown for comparison with those of Cs from hydrogenated W(110) surfaces [Fig. 7(b)]. In Fig. 7(b), the coverage of the preadsorbed hydrogen is about 0.5 ML, which corresponds to the β_2 adsorption state. Except for a shift to lower temperatures, the preadsorbed hydrogen does not cause any substantial change of the Cs-peak shapes. This indicates that the Cs atoms form an independent overlayer as on clean W(110), in agreement with LEED results. When the amount of preadsorbed H increases, the Cs peaks are shifted farther to lower temperatures, while the peak shapes are about the same. The shift of Cs peaks to lower temperature suggests that the presence of hydrogen on W(110) decreases the binding energy of the subsequently deposited Cs. This decrease is greater with increasing amounts of preadsorbed H.

2. *TDS of H_2*

Figures 8(a) and 8(b) show two series of hydrogen TDS spectra from Cs-covered H/W(110) and H/W(110), respectively. As is seen in the figure, the presence of the Cs overlayer does not substantially change the H-peak shape. The β_1 and β_2 adsorption states remain at about the same positions. Most likely, the presence of the Cs overlayer does not form any complex with the H underlayer and does not cause any obvious change in binding energy of it on W(110). The most probable configuration is one in which the small H atoms remain in their normal adsorption sites on W(110) and the subsequently deposited Cs atoms reside on top, in agreement with the LEED results.

E. Discussion

As we mentioned in the Introduction, one of the initiators of this work was the difference in WF variation of hydrogen on W(100) and W(110) surfaces. Adsorption of H_2 on a clean W(100) surface causes an increase of the WF,[1] while adsorption of H_2 on W(110) decreases the WF of the surface. According to the literature of the preceding decade,[16] hydrogen on W surfaces behaves in an electropositive manner. The increase of the WF on W(100) was attributed to a submergence of H atoms into the bulk of W, whereas the decrease of the WF on W(110) was at-

tributed to a deposition of H atoms on top of the outermost layer of the W(110) substrate.[16] However, in a recent study of hydrogen adsorption on W(100) and W(110) surfaces, it has been found that H atoms reside on top of the outermost plane of both W(100) and W(110) surfaces. Specifically, the H-W distances normal to relaxed surfaces are 1.15 Å for H/W(100), and 1.25 Å on the threefold site and ≥ 2.1 Å on the top site for H/W(110).[17] According to a theoretical work by Shustorovich,[23] chemisorption of electropositive adsorbates (such as alkali metals) will always decrease ϕ on all transition-metal surfaces, while chemisorption of electronegative adsorbates (such as H or halogens) can either increase or decrease ϕ, depending on the nature of the adsorbate and the type of the metallic substrate. The least electronegative adsorbates on the most highly dense surfaces are the most favorable to produce the paradoxical decrease of WF ($\Delta\phi < 0$). The smallest difference in adsorbate versus metallic substrate electronegativity proves to be the most likely to produce such a decrease in WF. Shustorovich's theoretical model[23] suggests that under chemisorption of an electronegative adatom on a transition-metal surface, the contributions to work-function change, $\Delta\phi$, are given by

$$\Delta\phi = \Delta\phi_{\text{ext}} + \Delta\phi_{\text{int}} , \tag{1}$$

where $\Delta\phi_{\text{int}}$ is the internal change of WF, which is due to changes in the surface dipole moment (surface polarization) of the substrate under chemisorption, and $\Delta\phi_{\text{ext}}$ is the external change in WF due to the dipole moment of the adsorbate. For an electronegative adsorbate $\Delta\phi_{\text{ext}} > 0$, under chemisorption of H (the least electronegative adsorbate), the charge transfer between H atoms and metal substrate is very small, i.e., there is a very small magnitude of $\Delta\phi_{\text{ext}} > 0$. For the most highly dense W(110) surface, $\Delta\phi_{\text{int}} < 0$, and if $|\Delta\phi_{\text{int}}| > \Delta\phi_{\text{ext}}$, then

$$\Delta\phi = \Delta\phi_{\text{int}} + \Delta\phi_{\text{ext}} < 0 . \tag{2}$$

This is an explanation for the WF decrease ($\Delta\phi < 0$) during adsorption of H_2 on the W(110) surface. Therefore, the small electronegativity of the H adsorbate and especially the small difference in electronegativity between H and W (2.20 and 2.36 on the Pauling scale, respectively) implies that the electronic charge transfer from the W substrate to the H adsorbate is very small. Also, the small electronegativity of H does not favor a strong interaction and/or a transfer of electronic charge between the Cs and the H underlayer, in contrast to the case of Cs and oxygen coadsorption on W surfaces.[1] Moreover, the H layer decreases the interaction between the Cs overlayer and the W substrate, and thus weakens the bond of Cs on W(110). This is consistent with the TDS measurements (Sec. IV D), which suggest that the presence of hydrogen on W(110) decreases the binding energy of the subsequently deposited Cs. Therefore, the main contribution of the almost neutral preadsorbed H on W(110) to the initial dipole moment of Cs adsorbate may be due to a displacement of the Cs overlayer towards the vacuum and consequently to an increase of Cs adsorbate-W substrate interlayer distance d.

According to a theoretical work by Wimmer *et al.*,[24] for a fixed coverage of Cs on W, but for different values of d, there is a strong dependence of $\Delta\phi$ on d. This dependence has been recently studied more systematically by Muscat and Batra.[25] This study suggests that the initial change of the WF in the ϕ-versus-Θ plot for an alkali metal on a metal substrate is more drastic with increasing adsorbate-substrate interlayer distance d. This implies that the initial dipole moment p_0 increases with increasing Cs-W interlayer distance d. As is seen in Fig. 9, the initial dipole moment of Cs on H/W(110), p_0, increases linearly with increasing area of the H_2 TDS peak of preadsorbed H_2 on W(110), which is proportional to Θ_H. Above 10 L of hydrogen exposure, which corresponds to about 1 ML of H on W(110) (where all the available sites are occupied) the change of p_0 is almost negligible. The induced dipole moment and depolarization effect of these dipoles with increasing Cs coverage (Θ_{Cs}) play an essential role in the initial decrease of $\phi(\Theta_{Cs})$.[26] The increase of the initial dipole moment with increasing amounts of preadsorbed H may cause an earlier dipolarization effect. This could be a reason for the shift of $\phi_{\min}$ to lower Cs coverages (Fig. 5). However, this is not the case, because the deviation from the initial constant slope of the WF curves in Fig. 5, which might be due to depolarization, occurs at about the same Cs coverage independently of the amount of H.

Muscat's and Batra's theory suggests that the onset of metallization of an alkali-metal overlayer is accompanied by an increased alkali-substrate interlayer distance d. The regain of charge by the overlayer is certainly faciliated if d increases at the coverage where metallization sets in. Therefore, for the same Θ_{Cs}, the increase of the Cs-W interlayer distance by the H is accompanied by an increase of the electron density in the Cs overlayer. Increasing electron density in the Cs overlayer with increasing amounts of preadsorbed H may cause an earlier

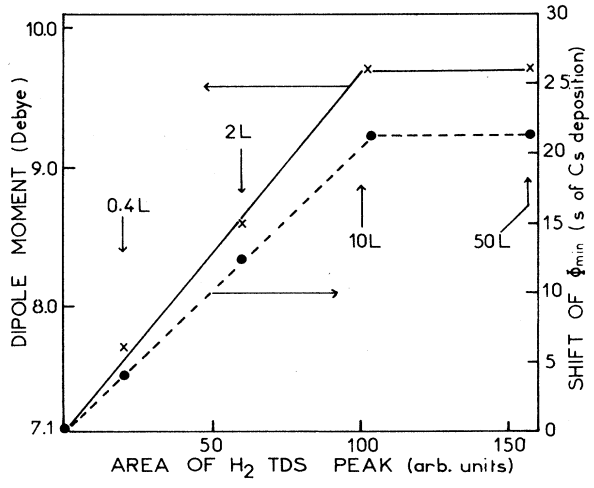

FIG. 9. Initial dipole moment p_0 and the shift of $\phi_{\min}$ of Cs on H-covered W(110) surfaces (calculated from Fig. 5) vs the area under the TDS peak of preadsorbed H_2W(110).

metallization in the Cs overlayer and thus an earlier occurrence of ϕ_{min}. Observed plasmons at coverages of alkali metals on metals right above ϕ_{min} suggest the appearance of nearly free electrons in the alkali-metal overlayer. This finding is in good agreement with the assumption about a metal-like overlayer.[27,28] Therefore, the shift of ϕ_{min} to lower Cs coverages with increasing amounts of preadsorbed H on W(110) (Fig. 5) could be attributed to an early metallization in the Cs overlayer with increasing amounts of preadsorbed H on W(110). An increase of the rate of metallization in the Cs overlayer with increasing amounts of preadsorbed H on W(110) can be seen in Fig. 5, where above ϕ_{min} the rate of WF increase with increasing Cs coverage is higher when the amount of preadsorbed H is greater. Figure 9 shows that the shift of ϕ_{min} increases almost linearly with increasing amounts of preadsorbed H on W, up to the completion of 1 ML ($\sim$10 L).

An analogous shift of ϕ_{min} has been reported. This shift occurred with increasing size of the deposited alkali-metal atoms (Na,K,Cs) on metal surfaces, such as Ru(001) and Ni(001).[29,27] Specifically, ϕ_{min} of the WF curves of Na, K, and Cs on Ni and Ru surfaces are shifted to lower coverage in the sequence of Na–K–Cs. Characteristic of the above measurements is the initial dipole moment increase from Na to Cs.[27] The surface dipole distance is greater for the bigger Cs adatoms than for the smaller Na adatoms. The observed shift of ϕ_{min} in the sequence of Na–K–Cs adsorbates on metals may be attributed to an early metallization of the layer with the larger alkali-metal adatoms. Most likely, the greater size of Cs atoms relative to Na atoms makes the appearance of free electrons start earlier in the Cs layer than in the Na layer.

Now let us discuss the increase of ϕ_{max} of Cs with increasing amounts of preadsorbed H on W(110) (Fig. 5). According to Lang's theory,[22] this could be attributed to an increase in the density of the saturated alkali-metal layer N_{max}. However, the LEED, AES, and TDS measurements in Secs. IV A, IV C, and IV D, respectively, indicate that N_{max} of Cs does not increase with increasing amounts of preadsorbed H on W(110). Considering again Muscat's and Batra's theory, the electron density of a saturated Cs layer on W(110) must be greater with increasing Cs-W interlayer distance d. As we mentioned earlier in this section, above ϕ_{min} the Cs overlayer starts to become metal-like. Therefore, the electron density of the Cs overlayer is greater in the presence of the H underlayer than without it. As the amount of preadsorbed H increases, the electron density in the saturated Cs overlayer becomes greater, with a resulting increase in ϕ_{max}.

Figure 10 shows the variation of ϕ_{min} and ϕ_{max} of the WF curves of Cs on H/W(110) (Fig. 5) versus the area under the TDS peak of preadsorbed H_2 on W(110) (the area is proportional to the preadsorbed Θ_H). The small linear decrease of ϕ_{min} is mainly due to the increase of p_0 with increasing Θ_H. ϕ_{max} increases almost exponentially with increasing Θ_H. This curve is quite similar to that of ϕ versus electron density n_e, in the adsorbed alkali-metal layers on a metal substrate, which has been reported by Wojciechowski.[26]

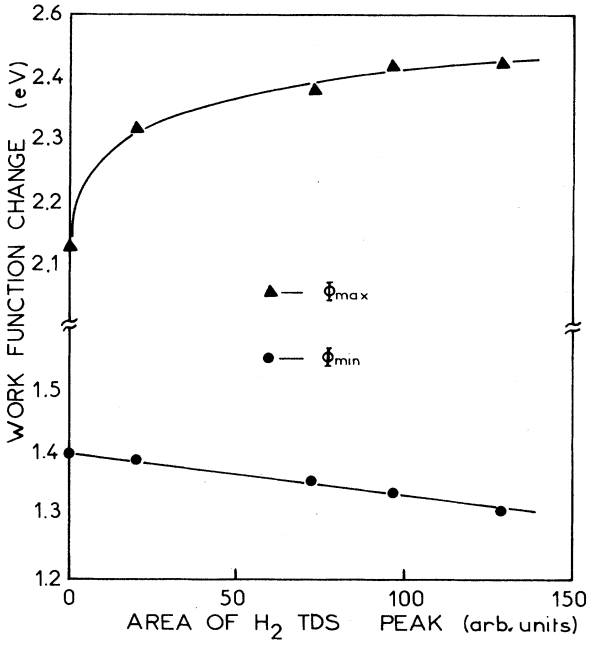

FIG. 10. Variation of ϕ_{min} and ϕ_{max} of the WF curves of Cs on H/W(110) surfaces (from Fig. 5) vs the area under the TDS peak of the preadsorbed H_2 on W(110).

At this point it is appropriate to correlate the present increase in the initial dipole moment of Cs versus increasing amounts of preadsorbed H on W(110) with the model proposed by Wimmer *et al.*[24] According to this model, the initial WF lowering upon cesiation of W arises from a complex multiple dipole formation mechanism. Essentially, the Cs valence electrons are polarized towards the W surface, leading to an increase in electronic charge in the interface region between the Cs and surface W atoms. We believe that, at early stages of Cs deposition, the increase in Cs-W distance by the almost-neutral H layer provides a spatial extension of the polarized Cs adatoms toward the W substrate. The result is an increase in the initial dipole moment and a further lowering of ϕ_{min}. Probably, at higher coverages, when the electronic communication between Cs adatoms occurs, the increase in the Cs-W distance by H weakens the Cs—W covalent bond, thus more electronic charge from the Cs-W interface is shifted into the Cs overlayer. The result is the enhancement of metallization in the Cs overlayer, with, as a consequence, the shift of ϕ_{min} and the increase in ϕ_{max}.

V. SUMMARY

The present work deals with a systematic experimental study of (a) Cs deposition on clean and H precovered W(110) surfaces, and (b) the adsorption of H_2 on clean and cesiated W(110) surfaces. The experiment was performed in a UHV system equipped with the surface techniques of LEED, AES, TDS, and WF measurements.

Deposition of Cs on clean W(110) at RT produces a single layer with a hcp structure at $\Theta_{max} \approx 0.37$ ML. It gives the characteristic WF curve of alkali metals on metals. Initially, the WF goes through a minimum value ϕ_{min} at $\Theta_{Cs} = 0.22$ ML, and subsequently increases to a maximum ϕ_{max} at saturation Cs coverage ($\Theta_{Cs} = 0.37$ ML).

During Cs deposition on H-covered W(110), the Cs atoms form an independent layer above the H layer. The presence of the H underlayer increases the ordering of the Cs atom, which produces a $p(2\times2)$ structure and a compressed hcp structure on 0.5 ML of H, whereas Cs forms an oblique (3×1) structure on 1 ML of H. The preadsorbed H causes (i) an increase in the initial dipole moment p_0, (ii) a lowering of ϕ_{min}, (iii) a shift of ϕ_{min} to smaller Θ_{Cs}, and (iv) an increase in ϕ_{max}. Hydrogen (the least electronegative) resides on top of the outermost plane of W(110), weakens the bond of the subsequently deposited Cs with the W substrate, and affects the structure of the Cs overlayer. The main effect of preadsorbed H is an increase in the W-Cs interlayer distance, which restricts the electronic interaction between the Cs and W substrates. According to Muscat and Batra,[25] an increase of Cs-W interlayer distance causes an increase in the initial surface dipole moments and in the electron density in the Cs overlayer. This is consistent with the lowering and shift of ϕ_{min} and also the increase of ϕ_{max}. This explanation is in agreement with Wimmer *et al.*,[24] theoretical work.

ACKNOWLEDGMENTS

We wish to thank Dr. M. Kamaratos, who helped with collection of some data.

[1]C. A. Papageorgopoulos and J. M. Chen, Surf. Sci. **39**, 313 (1973).
[2]J.-L. Desplat and C. A. Papageorgopoulos, Surf. Sci. **92**, 97 (1980).
[3]D. Edwards, Jr. and W. T. Peria, Appl. Surf. Sci. **1**, 419 (1979).
[4]C. A. Papageorgopoulos, Surf. Sci. **104**, 643 (1981).
[5]G. N. Hatsopoulos and E. P. Gyftopoulos, *Thermionic Energy Conversion* (MIT Press, Cambridge, Mass., 1979).
[6]M. H. Bakshi, P. Soukiassian, T. M. Gentle, and Z. Hurych, J. Vac. Sci. Technol. A **5**, 1428 (1987).
[7]C. A. Papageorgopoulos, S. Foulias, S. Kennou, and M. Kamaratos, Surf. Sci. **211/212**, 991 (1989).
[8]C. T. Campbell and B. E. Koel, Surf. Sci. **186**, 393 (1987).
[9]A. Pargellis and M. Seidl, Phys. Rev. B **25**, 4356 (1982).
[10]C. A. Papageorgopoulos and J. M. Chen, Surf. Sci. **39**, 283 (1973).
[1]M.-L. Ernst-Vidalis, M. Kamaratos, and C. A. Papageorgopoulos, Surf. Sci. **189/190**, 276 (1987).
[12]P. J. Schneider, K. H. Berkner, W. G. Graham, R. V. Pyle, and J. W. Strearns, Phys. Rev. B **23**, 941 (1981).
[13]M. Wada, R. V. Pyle, and J. S. Stearns, in *Production and Neutralization of Negative Ions and Beams (Brookhaven National Laboratory, Upton, New York)*, Proceedings of the Third International Symposium on Production and Neutralization of Negative Ions and Beams, AIP Conf. Proc. No. 111, edited by Krsto Prelec (AIP, New York, 1983), p. 247.
[14]P. W. Van Amersfoort, J. J. C. Geerlings, R. Rodink, E. H. A. Granneman, and J. Los, J. Appl. Phys. **59**, 241 (1986).
[15]J. P. Gauyacq and J. J. C. Geerlings, Surf. Sci. **182** 245 (1987).
[16]L. D. Schmidt, *Topics in Applied Physics,* edited by R. Gomer (Springer-Verlag, Berlin, 1975), Vol. 4, p. 80.
[17]H.-J. Herlt and E. Bauer, Surf. Sci. **175**, 336 (1986).
[18]C. J. Todd and T. N. Rhodin, Surf. Sci. **42**, 109 (1974).
[19]P. W. Tamm and L. D. Schmidt, J. Chem. Phys. **54**, 4775 (1971).
[20]A. G. Fedorus and A. G. Naumovets, Surf. Sci. **21**, 426 (1970).
[21]C. A. Papageorgopoulos, Phys. Rev. B **25**, 3740 (1981).
[22]N. D. Lang and W. Kohn, Phys. Rev. B **1**, 4555 (1970); **3**, 1215 (1971).
[23]E. Shustorovich, J. Phys. Chem. **86**, 3114 (1982).
[24]E. Wimmer, A. I. Freeman, I. R. Hishes, and A. M. Karo, Phys. Rev. B **28**, 3074 (1983).
[25]J. P. Muscat and I. Batra, Phys. Rev. B **34**, 2889 (1986).
[26]K. F. Wojciechowski, Surf. Sci. **55**, 246 (1976).
[27]G. Rangelov and L. Surnev, Surf. Sci. **185**, 457 (1987).
[28]B. Woratschek, W. Sesselmann, J. Küppers, G. Ertl, and H. Haberland, Phys. Rev. Lett. **55**, 1281 (1985).
[29]R. L. Gerlach and T. N. Rhodin, Surf. Sci. **19**, 403 (1970).

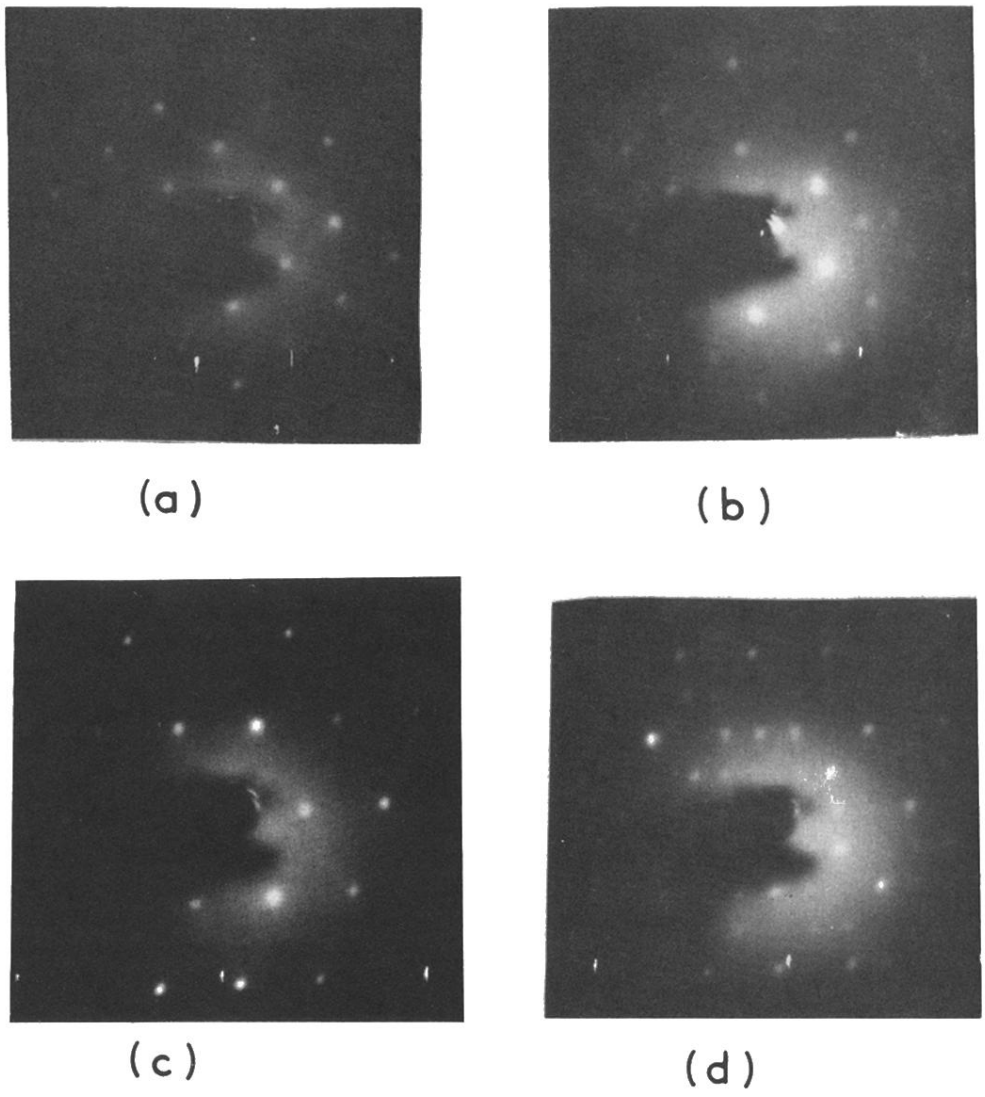

FIG. 2. LEED patterns of Cs on H-covered W(110) at RT. (a) $p(2\times2)$Cs, $\Theta_{Cs}\approx0.25$, $\Theta_H\approx0.5$ (95 eV). (b) hcp pattern with split beams $\Theta_{Cs}\approx0.37$, $\Theta_H\approx0.5$ [this pattern is similar to that of saturated Cs on clean W(110)] (85 eV). (c) Oblique (3×1)Cs, $\Theta_{Cs}\approx0.33$, $\Theta_H\approx1$ (95 eV). (d) Superposition of hcp and oblique (3×1)Cs, $0.33<\Theta_{Cs}<0.37$, $0.5<\Theta_H<1$, 100 eV.